ESC European Society of Cardiology

European Heart Journal - Cardiovascular Imaging (2023) **24**, 463–471
https://doi.org/10.1093/ehjci/jeac120

ORIGINAL PAPER

Distinct cardiovascular phenotypes are associated with prognosis in systemic sclerosis: a cardiovascular magnetic resonance study

Daniel S. Knight [1,2,3,4]*, Nina Karia[1,2,4], Alice R. Cole[5], Rory H. Maclean[5], James T. Brown[1,2,4], Ambra Masi[2,3], Rishi K. Patel [2,6], Yousuf Razvi [2,6], Liza Chacko[2,6], Lucia Venneri[2], Tushar Kotecha [1,2,3,4], Ana Martinez-Naharro[2,3,6], Peter Kellman [7], Ann M. Scott-Russell[8], Benjamin E. Schreiber[1], Voon H. Ong[5], Christopher P. Denton [5], Marianna Fontana [2,6], J. Gerry Coghlan[1,3†], and Vivek Muthurangu[4†]

[1]National Pulmonary Hypertension Service, Royal Free London NHS Foundation Trust, Pond Street, London, NW3 2QG, UK; [2]UCL Department of Cardiac MRI, University College London (Royal Free Campus), Rowland Hill Street, London, NW3 2PF, UK; [3]Department of Cardiology, Royal Free London NHS Foundation Trust, Pond Street, London, NW3 2QG, UK; [4]UCL Institute of Cardiovascular Science, University College London, Gower Street, London, WC1E 6BT, UK; [5]Centre for Rheumatology and Connective Tissue Diseases, UCL Medical School (Royal Free Campus), Rowland Hill Street, London, NW3 2PF, UK; [6]National Amyloidosis Centre, Division of Medicine, University College London, Rowland Hill Street, London, NW3 2PF, UK; [7]National Heart, Lung, and Blood Institute, National Institute of Health, 31 Center Dr, Bethesda, MD 20892, USA; and [8]Department of Rheumatology, Queen Alexandra Hospital, Cosham, Portsmouth, PO6 3LY, UK

Received 6 March 2022; revised 16 May 2022; accepted 13 June 2022; online publish-ahead-of-print 1 July 2022

Aims Cardiovascular involvement in systemic sclerosis (SSc) is heterogeneous and ill-defined. This study aimed to: (i) discover cardiac phenotypes in SSc by cardiovascular magnetic resonance (CMR); (ii) provide a CMR-based algorithm for phenotypic classification; and (iii) examine for associations between phenotypes and mortality.

Methods and results A retrospective, single-centre, observational study of 260 SSc patients who underwent clinically indicated CMR including native myocardial T1 and T2 mapping from 2016 to 2019 was performed. Agglomerative hierarchical clustering using only CMR variables revealed five clusters of SSc patients with shared CMR characteristics: dilated right hearts with right ventricular failure (RVF); biventricular failure dilatation and dysfunction (BVF); and normal function with average cavity (NF-AC), normal function with small cavity (NF-SC), and normal function with large cavity (NF-LC) sizes. Phenotypes did not co-segregate with clinical or antibody classifications. A CMR-based decision tree for phenotype classification was created. Sixty-three (24%) patients died during a median follow-up period of 3.4 years. After adjustment for age and presence of pulmonary hypertension (PH), independent CMR predictors of all-cause mortality were native T1 ($P < 0.001$) and right ventricular ejection fraction (RVEF) ($P = 0.0032$). NF-SC and NF-AC groups had more favourable prognoses ($P \leq 0.036$) than the other three groups which had no differences in prognoses between them ($P > 0.14$). Hazard ratios (HR) were statistically significant for RVF (HR = 8.9, $P < 0.001$), BVF (HR = 5.2, $P = 0.006$), and NF-LC (HR = 4.9, $P = 0.002$) groups. The NF-LC group remained significantly predictive of mortality after adjusting for RVEF, native T1, and PH diagnosis ($P = 0.0046$).

Conclusion We identified five CMR-defined cardiac SSc phenotypes that did not co-segregate with clinical data and had distinct outcomes, offering opportunities for a more precision-medicine based management approach.

* Corresponding author. Tel: (+44) 020 7433 2780, Fax: (+44) 020 7433 2817, E-mail: dan.knight@nhs.net
† J.G.C. and V.M. contributed equally to the manuscript and should be considered joint last authors.

Graphical Abstract

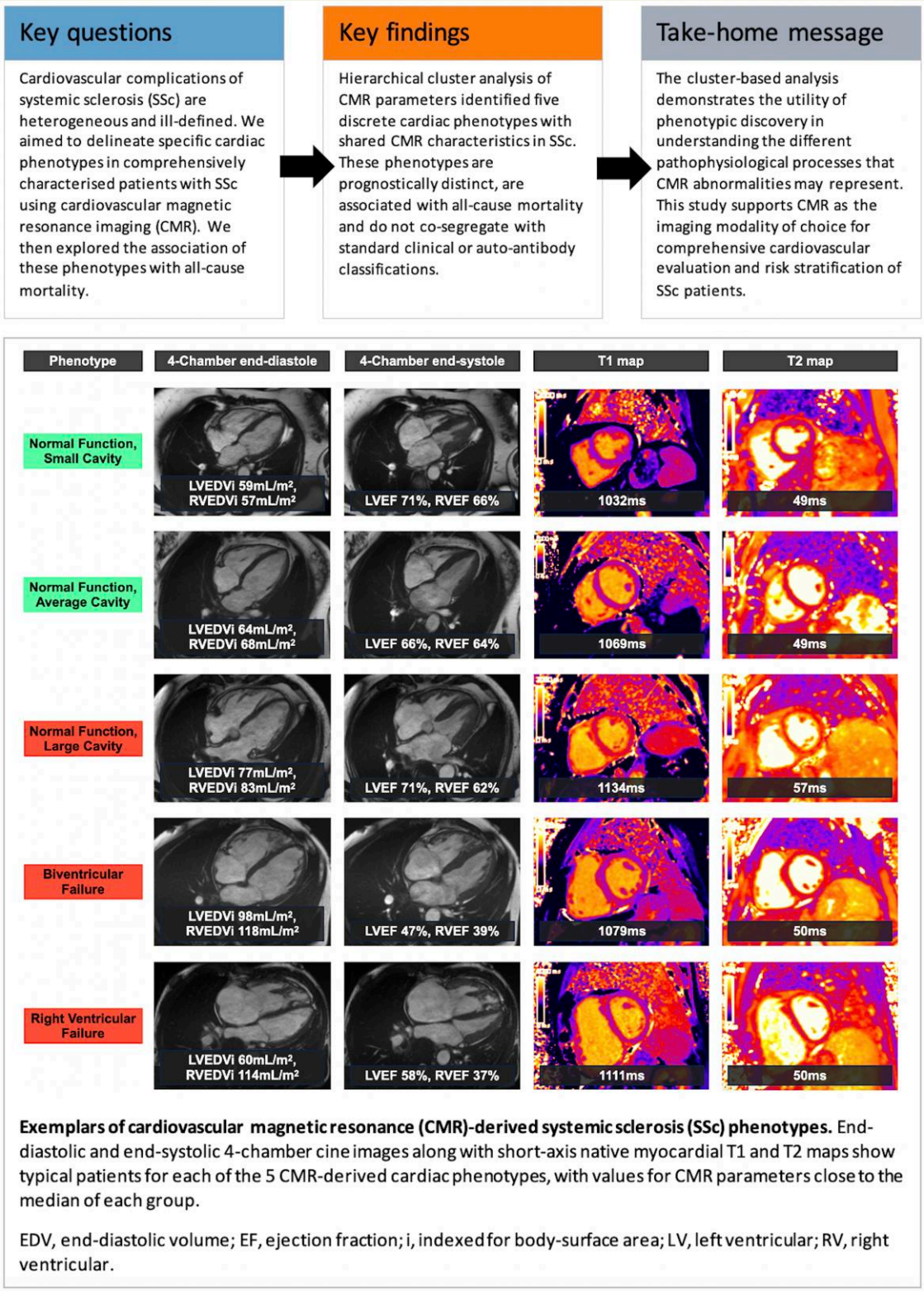

Exemplars of cardiovascular magnetic resonance (CMR)-derived systemic sclerosis (SSc) phenotypes. End-diastolic and end-systolic 4-chamber cine images along with short-axis native myocardial T1 and T2 maps show typical patients for each of the 5 CMR-derived cardiac phenotypes, with values for CMR parameters close to the median of each group.

EDV, end-diastolic volume; EF, ejection fraction; i, indexed for body-surface area; LV, left ventricular; RV, right ventricular.

Keywords cluster analysis • cardiovascular magnetic resonance • T1 mapping • prognosis • pulmonary hypertension • systemic sclerosis

Introduction

Systemic sclerosis (scleroderma; SSc) is a rare multi-system autoimmune rheumatic disease characterized by fibrosis, inflammation, and microvascular dysfunction.[1] Cardiac involvement is well-recognized in SSc and, when clinically manifest, is associated with a poor prognosis.[2–6] However, cardiovascular disease in SSc is not a simple binary phenomenon. Rather, it is heterogeneous and ill-defined, including diverse pathologies such as myocarditis, non-ischaemic fibrosis and scar, and pulmonary hypertension (PH).[7–9] Clearer identification of distinct cardiac phenotypes in SSc would help to better understand the disease and guide treatments and interventions. Unfortunately, this requires the evaluation of large patient cohorts which is difficult due to the rarity of SSc.

Our institution is a tertiary referral centre for SSc and related connective tissue diseases and we routinely perform cardiovascular magnetic resonance (CMR) when clinically assessing these patients. CMR is the most accurate and reproducible method of evaluating cardiac chamber size and function,[10] as well as myocardial tissue characterization for the assessment of myocardial oedema, scar, and diffuse fibrosis.[11] Importantly, this wealth of information allows more sophisticated methods of cardiac phenotype discovery to be used, including phenomapping. This clustering-based approach has been shown to identify novel phenotypes in other cardiac diseases that are not apparent using traditional statistical techniques. The aims of this study were: (i) to discover specific cardiac phenotypes in SSc by CMR using hierarchical cluster analysis; (ii) to provide a CMR-based algorithm for phenotypic classification; and (iii) to examine for associations between these CMR-derived cardiac phenotypes and mortality.

Methods

Patient population

This was a retrospective, single-centre, observational study of 265 consecutive patients with a diagnosis of SSc who underwent CMR including native myocardial T1 and T2 mapping at the Royal Free Hospital, London, United Kingdom (UK) from 2016 to 2019. All patients had symptoms (for example dyspnoea, chest pain, exercise intolerance) underlying the clinical indications for CMR studies to identify potential cardiovascular disease or follow-up known cardiovascular disease. All patients, including those with a concomitant overlap syndrome diagnosis, fulfilled the American College of Rheumatology/European League Against Rheumatism 2013 classification criteria for SSc.[12] Referrals originated from the Scleroderma Service at the Royal Free Hospital and from the National PH Service at the Royal Free Hospital (one of seven UK specialist centres for the management of adult PH).

The study complies with the Declaration of Helsinki and was approved by the East of England—Cambridge Central Research Ethics Committee (REC reference 21/EE/0037) who waived the necessity of a written consent according to the nature of the study (a register-based study with de-identified data and no active participation by study subjects).

Clinical data

Patient clinical histories, co-morbidities, and right heart catheterization (RHC) data were obtained from patient electronic records systems and specialist services databases by clinicians blinded to the patient outcomes. A validated SSc disease severity score at the time of the scan from 0 (no documented involvement) to 4 (end-stage disease) was derived as described previously.[13] Diagnoses of PH by RHC were made according to international guidelines.[14] Outcome was ascertained by checking the patient summary care record on the National Health Service (NHS) spine portal on 30th April 2021.

CMR protocol

CMR was performed on a 1.5T CMR scanner (Magnetom Aera, Siemens Healthcare, Erlangen, Germany). The CMR protocol and sequences have been described previously.[15] In summary, we acquired: (i) conventional cine imaging; (ii) mid short axis native T1 (modified 5s(3s)3s look-locker inversion recovery sequence after regional shimming) and T2 (single-shot T2-prepared sequence) maps[16]; (iii) late gadolinium enhancement (LGE) imaging using a phase-sensitive inversion recovery motion-corrected sequence following 0.1 mmoL/kg gadoterate meglumine; and (iv) Pixel-wise extracellular volume (ECV) parametric maps derived from pre- and post-contrast T1 maps, introduced at our institution from May 2016.[17] Post-contrast T1 maps were acquired at 15-min post-contrast administration. Patients with an estimated glomerular filtration rate < 30 mL/min/1.73 m^2 underwent a non-contrast study unless written informed consent was obtained for contrast administration.

CMR post-processing

All CMR studies were analysed using 'in-house' plug-ins for OsiriX MD version 9.0.1 (Pixmeo Sarl, Bernex, Switzerland).[18] All studies were reported by experienced clinical CMR observers blinded to patient outcomes (M.F., D.S.K., T.K., A.M.-N.).

End-diastolic volume (EDV), end-systolic volume (ESV), stroke volume (SV), ejection fraction (EF), and myocardial mass were calculated as previously described[19] with papillary muscles and trabeculae excluded from the blood pool. Bi-atrial areas were traced on a four-chamber cine image at end-systole. All cardiac volumes and dimensions were indexed (i) to body surface area. Myocardial mass was indexed to EDV to create mass-to-volume ratios (MVR) for the left and right ventricles.

Native myocardial T1 and T2 relaxation times along with myocardial ECV were measured by drawing a single region of interest within the interventricular septum on the mid-cavity short-axis maps remote from areas of LGE and the insertion points.[16]

Post-processing of LGE images was performed by visual assessment[20] with LGE patterns classified as: major ventricular insertion point (VIP), diffuse trabecular, diffuse subendocardial, focal subendocardial, mid-wall, subepicardial, and transmural. Minor VIP LGE was discounted.[21]

Statistics

All statistical resting was performed using R (RStudio 2021.09.02 using R 4.1.2). As most variables were non-normally distributed, groups are described by median and full range. Comparison of two groups was performed using the Wilcoxon rank sum test. For more than two groups, the Kruskal–Wallis test was used as an omnibus test with post-hoc pairwise comparison using the Wilcoxon rank sum test. Comparison of proportions was performed using Fisher's exact test with pairwise multiple tests. Adjustment for multiple comparisons was performed using the Benjamini and Hochberg method.

Prior to hierarchical clustering of continuous CMR variables and age, missing data were imputed using the *svdimpute* function (*pcaMethods*

package). In this method, missing values were imputed using regression with five eigenvectors as predictors. Redundant CMR metrics were then eliminated by first creating a correlation matrix and eliminating features where $r > 0.8$ (keeping the variable with the least correlations of $r > 0.8$). This resulted in the removal of both left ventricular (LV) and right ventricular (RV) ESVi. The final variables were standardized to mean = 0 and standard deviation = 1 prior to clustering.

Agglomerative hierarchical clustering was performed using the *hclust* function (*stats* package). The dissimilarity matrix was calculated using Euclidean distance and clusters were joined using Ward's method, which can separate clusters even in the presence of some noise. The optimal number of clusters was chosen using the *NBclust* function/package.[22] This method chooses the optimal number of clusters by calculating 27 different cluster validity indices and selecting the final optimal number of clusters using the majority rule. All clustering was performed blinded to clinical data and outcome data.

Univariable survival analyses for CMR variables, demographic variables and CMR-derived phenotypes were performed using Cox Proportional Hazards regression (*coxph* function from *survival* package) with hazard ratio (HR) reported per standard deviation change in metric for continuous data. The most predictive variables (decided by HR) from the biventricular volumetric indices, biventricular MVR, non-contrast mapping metrics, LGE and presence of pericardial effusion were then inputted into a multiple Cox Proportional Hazards regression adjusted for age and the presence of PH. Verification of proportional hazards assumption was performed using the *cox.zph* function (*survival* package). Differences in outcome between groups was assessed using Kaplan–Meier plots with both omnibus and pairwise Log-Rank test (with adjustment for multiple comparisons performed using the Benjamini and Hochberg method). The decision tree was created using the *rpart* function/package with splits based on the Gini index. For all tests, a P-value < 0.05 was considered statistically significant.

Results

Study population

Five patients were lost to follow-up having left the country since their CMR study and were excluded from the final analysis. Clinical details of the remaining 260 patients are summarized in Supplementary data online, *Table S1*. Median age was 59 (range 17–85) years and patients were predominantly female (208, 80%). Median time from SSc diagnosis to CMR was 9 years (range 0–47) and median disease severity score was 2 (range 1–4). The majority of SSc patients had limited (167, 64%) rather than diffuse (90, 35%) disease. Seventy-nine (30%) patients had an overlap connective tissue disease diagnosis. The main indication for CMR was myocardial tissue characterization followed by assessment for known or suspected PH, biventricular volumes and function quantification, and investigation for myocardial ischaemia (see Supplementary data online, *Table S2*).

Two-hundred seven (80%) patients had undergone RHC to diagnose the presence or absence of PH, 173 (84%) of whom had RHC performed within 1 year of the CMR study (median 5 days, range 0–349). Pulmonary hypertension was excluded in the remaining 53 (20%) patients by clinical evaluation and/or screening using the DETECT score (using a cut-off total risk score of ≤35), an evidence-based screening algorithm for the detection of SSc-associated pulmonary arterial hypertension.[23] One-hundred twelve (43%) patients had a diagnosis of PH, the majority of those (78 patients with PH, 70%) being pulmonary arterial hypertension (group 1). Further details of patients with SSc-associated PH are summarized in Supplementary data online, *Table S1*.

General CMR characteristics

CMR parameters are summarized in Supplementary data online, *Table S3*. Of the 245 patients (94%) who received contrast, 91 had significant LGE (37% of contrast studies). The distributions of LGE were: major VIP (44 patients, 48% of patients with significant LGE); diffuse trabecular (12, 13%); diffuse subendocardial (12, 13%); focal subendocardial (20, 22%); mid-wall (14, 15%); subepicardial (10, 11%); and transmural (7, 8%). Of the 26 patients with transmural or focal subendocardial LGE (1 patient having a combination of both), 20 (77%) had undergone either invasive (15 patients) or computed tomography (5 patients) coronary angiography. In these 20 patients, 14 (70%) had no evidence of significant coronary artery disease to account for the finding of ischaemic-pattern LGE.

Measurement of ECV was performed in 207 (80%) patients (median 32.1%, range 23.3–47.6%). The remaining patients did not have ECV measurement due to: (i) non-contrast study protocol (13, 5%); (ii) study performed prior to ECV mapping implementation at our CMR unit (25, 10%); and (iii) constraints specific to the clinical circumstances at the time of the scan (14, 5%).

Conventional analysis of CMR characteristics by clinically defined subgroups

Subgroup analyses according to the presence or absence of (i) PH and (ii) an overlap syndrome diagnosis are summarized in Supplementary data online, *Tables S4* and *S5*, respectively.

Patients with SSc-associated PH had higher RV volumes and mass, poorer RV function (all $P < 0.001$) and smaller LV volumes ($P = 0.037$) compared with SSc patients without PH. They also had significantly higher native myocardial T1 [1083 ms (983–1290) vs. 1063 ms (932–1195), $P < 0.001$] and T2 [51 ms (40–59) vs. 49 ms (41–59), $P = 0.0032$], higher myocardial ECV [32% (25–48) vs. 32% (23–43), $P = 0.0017$], and a greater prevalence of major VIP LGE (38% vs. 2%, $P < 0.001$) and pericardial effusions (36 vs. 20%, $P = 0.0048$).

Patients with SSc and an overlap syndrome diagnosis were younger (55 vs. 62 years, $P < 0.001$). There were no significant differences in CMR metrics of cardiac chamber size, function, or myocardial tissue characterization findings in patients with or without an overlap diagnosis.

Hierarchical cluster analysis

The amount of missingness of CMR metrics ranged from 2 (0.8%) to 6 (2.3%) patients (see Supplementary data online, *Table S6*). ECV was not included in the hierarchical cluster analysis due to the large amount of missingness for this metric. Cluster validity indices calculated from only the CMR data itself suggested that 5 was the optimal number of clusters. The dendrogram and associated heatmap divided into these five distinct clusters are shown in *Figure 1*.

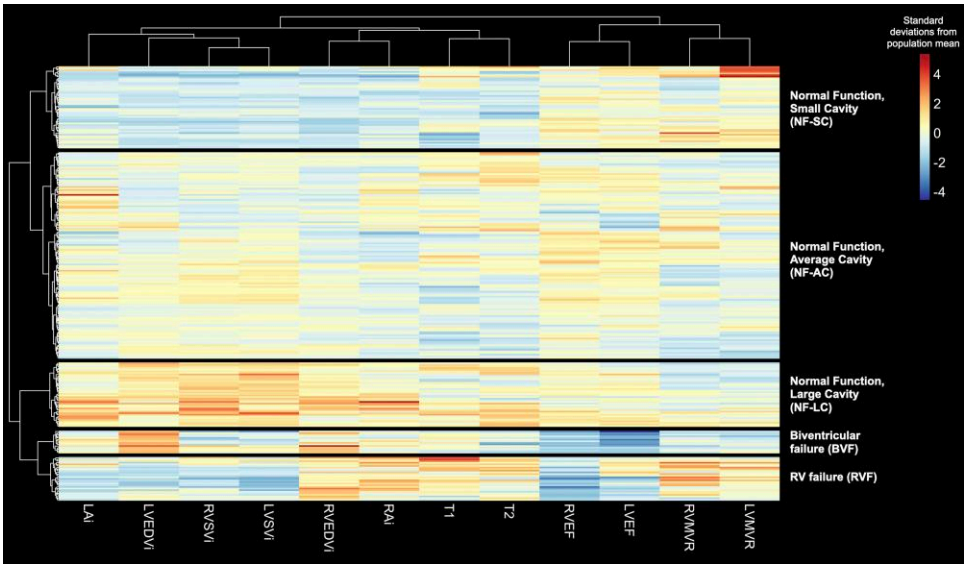

Figure 1 Agglomerative hierarchical clustering yielded five CMR-derived cardiac SSc phenotypes, the characteristics of which are displayed using a heatmap. Rows represent individual study participants; columns represent phenotypic variables. Red and blue indicate raised and low values of a phenotype relative to the study cohort average, respectively. HR, heart rate; LA, left atrial; RA, right atrial.

CMR characteristics of clusters

The CMR characteristics for each cluster (Graphical Abstract) are summarized as follows (reported in Supplementary data online, *Tables S7 and S8*):

- 'RV failure' (RVF) group: Dilated right hearts with the highest RV MVR [0.5 (0.2–0.8), $P \leq 0.0053$ vs. other groups], impaired RV systolic function [RVEF 39% (18–61%), $P < 0.001$ vs. other groups except the biventricular failure group], and high native myocardial T1 (1111 ms [983–1290 ms]). This group was associated with the highest prevalence of major VIP LGE (79%, $P < 0.001$ vs. all other groups) and a high proportion of pericardial effusions (59%, $P \leq 0.0062$ vs. the small and average cavity size groups).
- 'Biventricular failure' (BVF) group: Defined by large biventricular size, poor biventricular function [LVEF 37% (15–53%), $P < 0.001$ vs. other groups; RVEF 37% (26–52%), $P < 0.001$ vs. other groups except the RVF group], and high native myocardial T1 [1087 ms (1008–1127 ms)]. This group had the highest proportion of major non-VIP LGE (69%, $P \leq 0.0041$ vs. all other groups).
- 'Normal function, large cavity' (NF-LC) group: Characterized by biventricular dilation, preserved biventricular systolic function, biatrial dilatation, and high cardiac output. This group also had relatively high native myocardial T1 (1089 ms [990–1202], $P < 0.001$ except the BVF group) and T2 (53 ms [45–58], $P < 0.001$ except the RVF group) along with the second highest proportion of pericardial effusions (42%).
- 'Normal function, small cavity' (NF-SC) group: Relatively small cardiac chamber sizes (RVEDVi $P < 0.001$ vs. all groups, LVEDVi $P < 0.001$ vs. other groups except the RVF group) with normal ventricular function. This group had the lowest median native myocardial T1 (1050 ms, 932–1195 ms).
- 'Normal function, average cavity' (NF-AC): The largest group (128 patients, 49% of the overall cohort) consists of cardiac chamber sizes and native myocardial T1 (1066 ms, 946–1180 ms) in the mid-range for the overall population with normal biventricular systolic function.

Clinical phenotype associations with clusters

Clinical associations with clusters are reported in Supplementary data online, Tables S9–S12. There were no significant differences in the distributions of patients with limited SSc, diffuse SSc or an overlap connective tissue disease syndrome across the five phenogroups. There were significantly more men in the BVF group ($P = 0.009$). Other than a higher proportion of anticentromere antibody positivity in the three normal function groups vs. the BVF group ($P \leq 0.021$), there were no other significant differences in antibody status across the clusters. There were no significant differences in the proportions of patients with a history of ischaemic heart disease between the clusters ($P < 0.26$).

The RVF group predominantly consisted of patients with SSc-associated PH (92%) with significantly higher mean pulmonary arterial pressures vs. all other groups (47 mmHg [17–69], $P \leq 0.014$). However, most patients in the overall population with a diagnosis of SSc-associated PH were evenly distributed across the other four clusters (ranging from 33–50% in each cluster) with no significant differences in mean pulmonary artery pressure amongst those phenotypes.

All patients in the BVF group had myocardial tissue characterization as an indication for their CMR ($P \leq 0.03$ vs. all other groups), whereas the RVF group had a significantly smaller proportion of patients undergoing CMR for this reason ($P \leq 0.027$ vs. all other groups). Six patients in the BVF group had potentially ischaemic-pattern (focal subendocardial and/or transmural) LGE; five (83%) of these patients had angiographic data available, and none of whom had an underlying coronary culprit to account for the LGE.

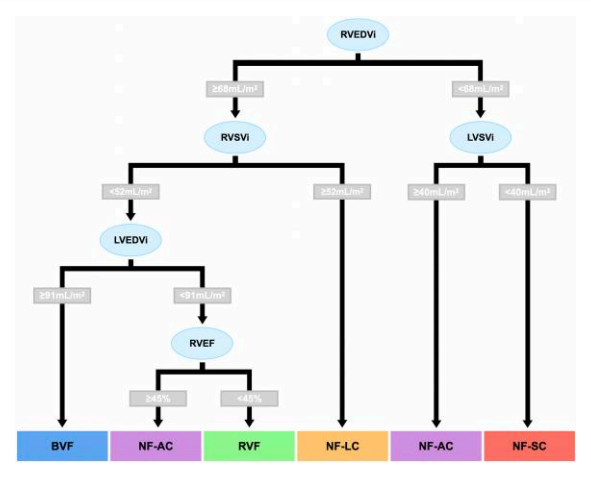

Figure 2 A CMR-based decision tree using biventricular volumetric data was derived to enable patients to be easily classified into their respective group membership.

Decision tree for simple clustering

In order to aid in future validation of these clusters, a decision tree was created that allowed simpler allocation of group membership (*Figure 2*). The optimum attributes were all related to ventricular volumes and function. The accuracy for prediction of group membership in the overall cohort was 82% (confidence intervals = 77–86%). When excluding patients with a diagnosis of PH, the accuracy for prediction of group membership was 85% (confidence intervals = 78–90%).

Predictors of mortality

Sixty-three (24%) patients died during a median follow-up period of 3.4 years (range 0.1–5.3 years). One-year and three-year survival was 92 and 76%, respectively.

Clinical SSc phenotypes and mortality

The presence of SSc-associated PH was associated with a significantly increased risk of death ($P < 0.001$; Supplementary data online, *Figure S1*). There was no difference in mortality between patients with limited vs. diffuse cutaneous SSc ($P = 0.51$; Supplementary data online, *Figure S1*). Patients with SSc and a concomitant overlap syndrome diagnosis also did not have a significantly different outcome compared to those without overlap syndromes ($P = 0.12$; Supplementary data online, *Figure S1*).

CMR predictors of mortality

Individual CMR variables predictive of all-cause mortality on univariable Cox analysis are shown in Supplementary data online, *Figure S2*. The following CMR predictors of mortality were entered into multivariable Cox analysis, none of which violated the proportional hazards assumption ($P > 0.1$): RV MVR, RVEF, native myocardial T1, presence of pericardial effusion and major VIP LGE. After adjustment for age and the presence of PH, the only independent predictors of mortality were native myocardial T1 ($P < 0.001$) and RVEF ($P = 0.0032$).

Associations between cardiac CMR-SSc phenotype and mortality

Kaplan-Meier curves for the five groups identified by hierarchical cluster analysis of CMR variables are shown in *Figure 3A*. The NF-SC and NF-AC groups had similar prognoses ($P = 0.27$), with both having more favourable prognoses than the three other groups ($P \leq 0.036$) by pairwise Log-Rank testing. There was no difference in prognoses between the BVF, RVF, and NF-LC groups ($P > 0.14$). On Cox regression, HRs (compared to the NF-SC group) were statistically significant for the RVF (HR = 8.9, $P < 0.001$), BVF (HR = 5.2, $P = 0.006$) and NF-LC (HR = 4.9, $P = 0.002$) groups, with no violation of the proportional hazards assumption ($P = 0.63$). These remained significant after independently adjusting for native T1 and diagnosis of PH ($P \leq 0.013$). After adjusting for RVEF, the RVF ($P = 0.01$), and NF-LC ($P = 0.001$) groups remained significant predictors of death. Adjusting for RVEF, native T1 and diagnosis of PH together resulted in only the NF-LC group remaining significantly predictive of mortality ($P = 0.0046$).

Figure 3B shows that the Kaplan-Meier curves using the decision tree-based grouping were similar to the actual hierarchical clustering-derived groupings.

Discussion

In this study, we evaluated a large cohort of clinically and haemodynamically well-characterized patients with SSc undergoing CMR. Using hierarchical cluster analysis, we discovered five CMR-defined cardiac phenotypes in SSc that do not co-segregate with existing clinical subgroup classifications or autoantibody status. Importantly, these CMR-defined cardiac phenotypes are associated with different outcomes and are independently predictive of mortality. Conversely, conventional clinical sub-classifications of SSc (namely: (i) limited vs. diffuse cutaneous SSc and (ii) the presence or absence of a concomitant overlap syndrome) were not of prognostic significance in our cohort. Thus, we believe that CMR offers an important tool for phenotype discovery, allowing a better understanding of SSc-associated cardiovascular disease and potentially helping guide both the treatment and risk stratification of these patients.

Although studies have demonstrated abnormal cardiac function[2,24,25] and tissue characteristics[3–6] in SSc patients, these simple comparisons do not adequately reflect the complexity and spectrum of cardiovascular pathology within this patient population. Therefore, we used hierarchical cluster analysis of CMR parameters to identify distinct cardiac phenotypes in SSc. This method does not use any additional background clinical/outcome data to generate clusters and is an unbiased method of discovering novel phenotypes based only on CMR data. The five phenotypes identified using this method were not associated with clinically defined SSc classifications or specific SSc-associated autoantibodies. This suggests that CMR-defined phenotypes can provide new insights into cardiac disease in SSc.

The poor outcomes in the RVF and BVF groups are unsurprising as ventricular failure is a recognized prognostic marker in many cardiovascular diseases. Although the RVF group consisted mainly of patients with PH, most patients with PH in the overall cohort were distributed across the other four phenotypes. This group actually

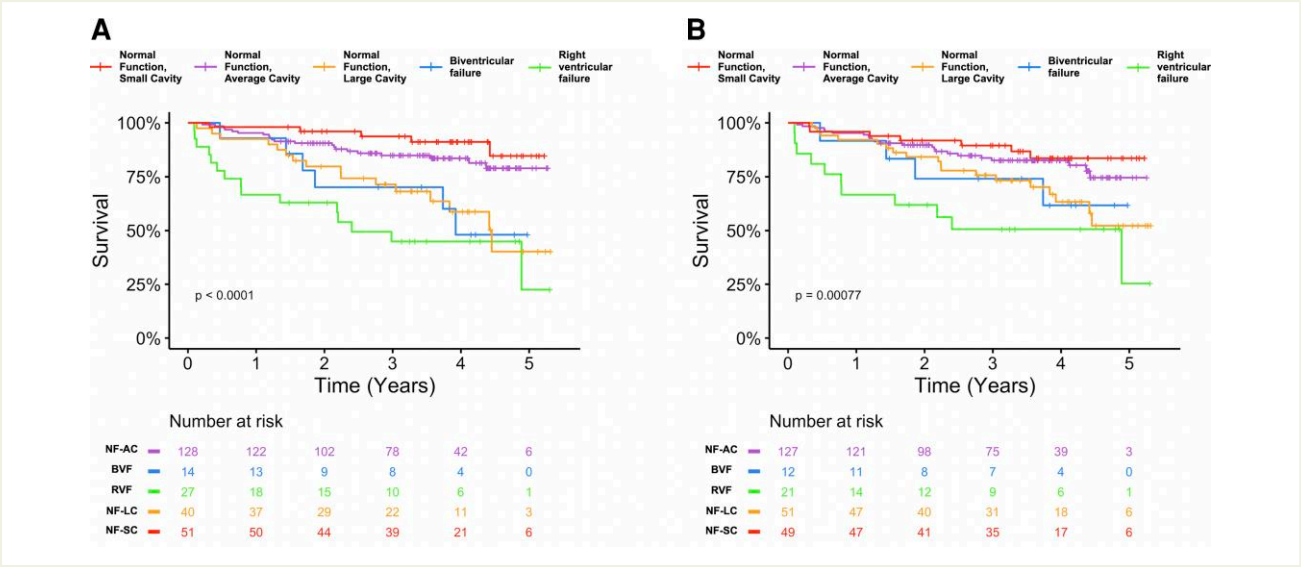

Figure 3 Kaplan–Meier curves for all-cause mortality stratified: (*A*) by hierarchical clustering-derived groupings; (*B*) using the decision tree-based grouping. The Kaplan–Meier curves using the decision tree-based groupings (*B*) were similar to those using the actual hierarchical clustering-derived groupings (*A*). Statistically significant values: $P < 0.05$.

represented those with the most adverse pulmonary haemodynamics and most underwent CMR for assessment of PH. Indeed, the elevated native T1 in the RVF group is in keeping with other studies of LV myocardial T1 metrics in patients with PH which show correlations between pulmonary haemodynamics with the degree of T1 elevation.[26] This may represent fibrosis and cardiomyocyte atrophy in the underfilled LV in this condition. The BVF group probably represents advanced or 'burnt out' SSc-related heart muscle disease, as indicated by the high myocardial T1, normal myocardial T2 (suggestive of no myocardial oedema) and the high prevalence of non-VIP myocardial scar. This is reflected by the fact the commonest indication for CMR in this group was myocardial tissue characterization. Interestingly, this group had the highest proportion of men, a known risk factor for LV dysfunction in SSc.[27] Identifying this cluster supports the notion that trials of advanced heart failure therapies and implantable cardioverter defibrillators could be focused upon this SSc phenotype. Both these groups have low RVEF and high T1, partly explaining why these metrics are powerfully predictive of mortality in the overall cohort.

Probably, the most intriguing group of patients are those with large cavity size and normal biventricular systolic function (NF-LC group). The outcomes in this group are poor and not statistically different from the RVF and BVF groups, even though they have normal cardiac function. Moreover, membership of this group is prognostic even when adjusted for RVEF, T1 and the presence of PH. This group, to our knowledge, has not previously been described, demonstrating the power of cluster analysis for prognostically significant phenotype discovery. These patients could be described as having a hyperdynamic state with dilated atria and ventricles and a significantly higher cardiac output than other groups. A possible unifying cause could be systemic inflammation, reinforced by the high prevalence of pericardial effusions in the absence of biventricular systolic dysfunction. The NF-LC group also exhibited high myocardial T2 compared to other groups, suggesting myocardial oedema. However, the distribution of T2 in this group shows that many patients were not overtly myocarditic by conventional diagnostic criteria. A potential explanation could be a low-level of myocardial inflammation possibly accompanying a systemic inflammatory state. Abnormalities of myocardial T2 in SSc patients are also known to be predictive of ventricular arrhythmia, a potential reason underlying the poor prognosis in the NF-LC group.[28] The last two phenotypes (NF-AC and NF-SC) had the most favourable prognoses and constituted the largest proportion of SSc patients. Both groups had 'relatively' normal hearts with normal function and tissue characteristics, and better outcomes than the other three groups.

A tendency to high native myocardial T1 is a finding that is common to all three phenotypes with the poorest prognoses, helping to explain why this is a powerful CMR predictor of mortality in the overall patient cohort. However, whilst important for prognosis, the finding of a high T1 value in isolation may not necessarily guide the CMR reader to a particular underlying pathophysiology. We believe that the differences in outcomes in these distinct clusters demonstrate the utility of more sophisticated forms of phenotypic discovery. However, an important area of future work will be investigating if these groups and their associated prognoses are applicable to new patients. For these reasons, we created a decision tree to enable patients to be more easily classified according to data from clinical CMR studies. This tool is advantageous as it relies solely on volumetric data which is acquired routinely and with little variation in clinical CMR practice. Furthermore, whilst previous studies have suggested a prognostic signal with the presence of LGE in SSc patients, our decision tree does not require post-contrast data for patient classification.[29] Reassuringly, we also found that outcomes using the decision tree-based grouping method were similar to those from the actual hierarchical clustering-derived groupings, irrespective of the presence or absence of PH in the study cohort. Since only

volumetric data are utilized in the decision tree, future work using three-dimensional echocardiography could similarly be performed for the multi-modality assessment of cardiovascular SSc phenotypes.

Limitations

The main limitation of the study was potential referral bias due to patient recruitment from a single site. This led to a study cohort that may not necessarily reflect the general SSc patient population. For example, our study cohort is over-represented by patients with PH, a complication that is typically present in 8 to 12% of SSc patients.[30] Nonetheless, we did attempt to mitigate for this by adjusting for the diagnosis of PH when assessing the prognostic utility of individual CMR variables and the different phenotypic groups. Unfortunately, because of the large proportion of patients with PH it was not possible to exclude these patients and robustly redo our cluster analysis. Nevertheless, we did test our decision tree algorithm on patients without PH and found high accuracy. Whilst the majority of PH diagnoses were in group 1 (70%), we grouped together all PH groups for our analysis. However, any PH diagnosis is known to confer a poorer prognosis when present. Our patient cohort was also older than previously described populations and thus we adjusted for age in our analyses. It should be noted that all SSc patients who underwent CMR in a 4-year period at our institution were included in the study other than five individuals who moved out of the country and hence were lost to follow-up. Therefore, this large cohort is representative of a 'real-world' cohort of patients with a confirmed diagnosis of SSc referred for a CMR in our clinical practice. However, replication and validation in independent cohorts is essential to determine if these phenotypes are generalizable to other groups of SSc patients. Furthermore, the goals for future studies include defining CMR features based on SSc diagnosis ideally as the first step, then distinguishing primary SSc cardiovascular involvement from comorbidity, non-SSc heart disease and the effects of PH. These are likely to be best assessed in prospective multi-centre patient cohorts.

The second major limitation was missingness in contemporaneous data due to the retrospective design of the study and inhomogeneities in the study protocol. For instance, blood test results that may provide complementary information to the CMR data, such as troponin and brain natriuretic peptide (BNP) levels, were not available in all patients. ECV also exhibited a significant missingness (20% compared with 0.8–2.3% for all other CMR metrics) and haematocrit values in some cases taken from the clinic visit closest to the CMR study. For these reasons ECV was not included in our hierarchical cluster analysis. LGE was also not included in the cluster analysis given that all other metrics were continuous data. In this regard, however, non-VIP LGE was not prognostic in our cohort and the majority of non-VIP LGE was found in patients in the BVF group. Standard metrics of disease duration, such as first non-RP manifestation, were unavailable for the entire cohort as some patients were referred from external centres. Measures of diastolic function and strain are unavailable, but previous studies have shown strain metrics may provide incremental prognostic value.[31,32] Therefore, future studies that have broader inclusion of contemporaneous multi-modality data (including electrocardiograms, echocardiograms, pulmonary function tests and coronary angiographic data) may also be important in refining cardiac phenotypes in SSc patients.

Conclusion

We have defined five CMR-derived phenotypes using hierarchical cluster analysis that are prognostically distinct, associated with all-cause mortality and do not co-segregate with standard clinical classifications. Patients can be classified using an algorithm only requiring routinely acquired CMR-derived volumetric indices. Abnormalities of native myocardial T1 and RVEF, both independently predictive of mortality even after adjustment for the presence of PH, were evident in phenotypes with the poorest prognoses. Phenotype discovery helps to delineate the spectrum of cardiovascular disease in SSc and enables a better understanding of the different pathophysiological processes that abnormal CMR metrics may represent. This confers opportunities for greater homogeneity of patient cohorts for clinical trials and a more precision medicine-based approach to treatment. Overall, this study supports CMR as the imaging modality of choice for the comprehensive cardiovascular evaluation and risk stratification of SSc patients.

Supplementary data

Supplementary data are available at *European Heart Journal—Cardiovascular Imaging* online.

Acknowledgements

In memory of Dr Karl Norrington.

Funding

D.S.K. is supported by a British Heart Foundation (BHF) Clinical Research Leave Fellowship (FS/CRLF/20/23004) and by the National Institute for Health Research (NIHR) University College London Hospitals (UCLH) Biomedical Research Centre (BRC). M.F. is supported by a BHF Intermediate Fellowship (FS/18/21/33447).

Conflict of interest: The authors declare that there are no conflicts of interest in relation to the work in this manuscript. Non-conflicting relationships with industry are as follows: D.S.K. reports consulting fees, speaker bureau fees and research funding from Johnson & Johnson. A.M.S-R. reports sponsorship from Janssen, Abbvie and Pfizer. B.E.S. reports consulting fees, speaker bureau fees and research funding from Johnson & Johnson, and speaker fees from GSK. C.P.D. reports personal fees from Acceleron, Corbus, Boehringer Ingelheim, Horizon, Johnson & Johnson, Roche, Sanofi, and grants and personal fees from CSL Behrin, GSK and Inventiva. J.G.C. reports consulting fees from Acceleron, consulting and speaker bureau fees from Bayer, GSK and Johnson & Johnson, and research funding from Johnson & Johnson.

Data availability

All data are incorporated into the article and its online supplementary material. The study dataset and software code will be made available to other researchers for purposes of reproducing the results or replicating the procedure upon reasonable request to the corresponding author, subject to institutional and ethical committee approvals.

References

1. Denton CP, Khanna D. Systemic sclerosis. *Lancet* 2017;**390**:1685–99.
2. Tyndall AJ, Bannert B, Vonk M, Airò P, Cozzi F, Carreira PE, *et al.* Causes and risk factors for death in systemic sclerosis: a study from the EULAR Scleroderma trials and research (EUSTAR) database. *Ann Rheum Dis* 2010;**69**:1809–15.
3. Ntusi NA, Piechnik SK, Francis JM, Ferreira VM, Rai AB, Matthews PM, *et al.* Subclinical myocardial inflammation and diffuse fibrosis are common in systemic sclerosis–a clinical study using myocardial T1-mapping and extracellular volume quantification. *J Cardiovasc Magn Reson* 2014;**16**:21.
4. Poindron V, Chatelus E, Canuet M, Gottenberg JE, Arnaud L, Gangi A, *et al.* T1 mapping cardiac magnetic resonance imaging frequently detects subclinical diffuse myocardial fibrosis in systemic sclerosis patients. *Semin Arthritis Rheum* 2020;**50**:128–34.
5. Thuny F, Lovric D, Schnell F, Bergerot C, Ernande L, Cottin V, *et al.* Quantification of myocardial extracellular volume fraction with cardiac MR imaging for early detection of left ventricle involvement in systemic sclerosis. *Radiology* 2014;**271**:373–80.
6. Terrier B, Dechartres A, Gouya H, Ben Arfi M, Bérézne A, Régent A, *et al.* Cardiac intravoxel incoherent motion diffusion-weighted magnetic resonance imaging with T1 mapping to assess myocardial perfusion and fibrosis in systemic sclerosis: association with cardiac events from a prospective cohort study. *Arthritis Rheumatol* 2020; **72**:1571–80.
7. Campo A, Mathai SC, Le Pavec J, Zaiman AL, Hummers LK, Boyce D, *et al.* Hemodynamic predictors of survival in scleroderma-related pulmonary arterial hypertension. *Am J Respir Crit Care Med* 2010;**182**:252–60.
8. Kahan A, Coghlan G, McLaughlin V. Cardiac complications of systemic sclerosis. *Rheumatology (Oxford)* 2009;**48**:iii45–8.
9. Ross L, Prior D, Proudman S, Vacca A, Baron M, Nikpour M. Defining primary systemic sclerosis heart involvement: a scoping literature review. *Semin Arthritis Rheum* 2019;**48**:874–87.
10. Hundley WG, Bluemke DA, Finn JP, Flamm SD, Fogel MA, Friedrich MG, *et al.* ACCF/ACR/AHA/NASCI/SCMR 2010 expert consensus document on cardiovascular magnetic resonance: a report of the American College of Cardiology foundation task force on expert consensus documents. *J Am Coll Cardiol* 2010;**55**:2614–62.
11. Leiner T, Bogaert J, Friedrich MG, Mohiaddin R, Muthurangu V, Myerson S, *et al.* SCMR position paper (2020) on clinical indications for cardiovascular magnetic resonance. *J Cardiovasc Magn Reson* 2020;**22**:76.
12. van den Hoogen F, Khanna D, Fransen J, Johnson SR, Baron M, Tyndall A, *et al.* 2013 Classification criteria for systemic sclerosis: an American College of Rheumatology/European league against rheumatism collaborative initiative. *Arthritis Rheum* 2013;**65**: 2737–47.
13. Medsger TA Jr, Silman AJ, Steen VD, Black CM, Akesson A, Bacon PA, *et al.* A disease severity scale for systemic sclerosis: development and testing. *J Rheumatol* 1999;**26**: 2159–67.
14. Galie N, Humbert M, Vachiery JL, Gibbs S, Lang I, Torbicki A, *et al.* 2015 ESC/ERS guidelines for the diagnosis and treatment of pulmonary hypertension: the joint task force for the diagnosis and treatment of pulmonary hypertension of the European Society of Cardiology (ESC) and the European Respiratory Society (ERS): endorsed by: Association for European Paediatric and Congenital Cardiology (AEPC), International Society for Heart and Lung Transplantation (ISHLT). *Eur Heart J* 2016;**37**:67–119.
15. Kotecha T, Knight DS, Razvi Y, Kumar K, Vimalesvaran K, Thornton G, *et al.* Patterns of myocardial injury in recovered troponin-positive COVID-19 patients assessed by cardiovascular magnetic resonance. *Eur Heart J* 2021;**42**:1866–78.
16. Messroghli DR, Moon JC, Ferreira VM, Grosse-Wortmann L, He T, Kellman P, *et al.* Clinical recommendations for cardiovascular magnetic resonance mapping of T1, T2, T2* and extracellular volume: a consensus statement by the society for cardiovascular magnetic resonance (SCMR) endorsed by the European association for cardiovascular imaging (EACVI). *J Cardiovasc Magn Reson* 2017;**19**:75.
17. Kellman P, Wilson JR, Xue H, Ugander M, Arai AE. Extracellular volume fraction mapping in the myocardium, part 1: evaluation of an automated method. *J Cardiovasc Magn Reson* 2012;**14**:63.
18. Rosset A, Spadola L, Ratib O. Osirix: an open-source software for navigating in multidimensional DICOM images. *J Digit Imaging* 2004;**17**:205–216.
19. Knight DS, Zumbo G, Barcella W, Steeden JA, Muthurangu V, Martinez-Naharro A, *et al.* Cardiac structural and functional consequences of amyloid deposition by cardiac magnetic resonance and echocardiography and their prognostic roles. *JACC Cardiovasc Imaging* 2019;**12**:823–33.
20. Schulz-Menger J, Bluemke DA, Bremerich J, Flamm SD, Fogel MA, Friedrich MG, *et al.* Standardized image interpretation and post-processing in cardiovascular magnetic resonance—2020 update: society for cardiovascular magnetic resonance (SCMR): board of trustees task force on standardized post-processing. *J Cardiovasc Magn Reson* 2020;**22**:19.
21. Joy G, Artico J, Kurdi H, Seraphim A, Lau C, Thornton GD, *et al.* Prospective case-control study of cardiovascular abnormalities 6 months following mild COVID-19 in healthcare workers. *JACC Cardiovasc Imaging* 2021;**14**:2155–66.
22. Charrad M, Ghazzali N, Boiteau V, Niknafs A. Nbclust: an R package for determining the relevant number of clusters in a data set. *J Stat Softw* 2014;**61**:1–36.
23. Coghlan JG, Denton CP, Grunig E, Bonderman D, Distler O, Khanna D, *et al.* Evidence-based detection of pulmonary arterial hypertension in systemic sclerosis: the DETECT study. *Ann Rheum Dis* 2014;**73**:1340–9.
24. Saito M, Wright L, Negishi K, Dwyer N, Marwick TH. Mechanics and prognostic value of left and right ventricular dysfunction in patients with systemic sclerosis. *Eur Heart J Cardiovasc Imaging* 2018;**19**:660–7.
25. van Wijngaarden SE, Boonstra M, Bloem B, Cassani D, Tanner FC, Jordan S, *et al.* Clinical and echocardiographic associates of all-cause mortality and cardiovascular outcomes in patients with systemic sclerosis. *JACC Cardiovasc Imaging* 2019;**12**: 2273–2276.
26. Homsi R, Luetkens JA, Skowasch D, Pizarro C, Sprinkart AM, Gieseke J, *et al.* Left ventricular myocardial fibrosis, atrophy, and impaired contractility in patients with pulmonary arterial hypertension and a preserved left ventricular function: a cardiac magnetic resonance study. *J Thorac Imaging* 2017;**32**:36–42.
27. Allanore Y, Meune C, Vonk MC, Airo P, Hachulla E, Caramaschi P, *et al.* Prevalence and factors associated with left ventricular dysfunction in the EULAR Scleroderma trial and research group (EUSTAR) database of patients with systemic sclerosis. *Ann Rheum Dis* 2010;**69**:218–21.
28. Mavrogeni S, Gargani L, Pepe A, Monti L, Markousis-Mavrogenis G, De Santis M, *et al.* Cardiac magnetic resonance predicts ventricular arrhythmias in scleroderma: the scleroderma arrhythmia clinical utility study (SAnCtUS). *Rheumatology (Oxford)* 2020;**59**:1938–48.
29. Mousseaux E, Agoston-Coldea L, Marjanovic Z, Stanciu R, Deligny C, Perdrix L, *et al.* Left ventricle replacement fibrosis detected by CMR associated with cardiovascular events in systemic sclerosis patients. *J Am Coll Cardiol* 2018;**71**:703–5.
30. Condliffe R, Kiely DG, Peacock AJ, Corris PA, Gibbs JS, Vrapi F, *et al.* Connective tissue disease-associated pulmonary arterial hypertension in the modern treatment era. *Am J Respir Crit Care Med* 2009;**179**:151–7.
31. Butcher SC, Vos JL, Fortuni F, Galloo X, Liem SIE, Bax JJ, *et al.* Evaluation of left cardiac chamber function with cardiac magnetic resonance and association with outcome in patients with systemic sclerosis. *Rheumatology (Oxford)* 2022:keac256. doi:10.1093/rheumatology/keac256.
32. Vos JL, Butcher SC, Fortuni F, Galloo X, Rodwell L, Vonk MC, *et al.* The prognostic value of right atrial and right ventricular functional parameters in systemic sclerosis. *Front Cardiovasc Med* 2022;**9**:845359.